GEOLOGY | THE GEOLOGICAL SOCIETY OF AMERICA®

https://doi.org/10.1130/G47406.1

Manuscript received 19 January 2020
Revised manuscript received 5 March 2020
Manuscript accepted 18 March 2020

Published online 12 May 2020

Onset of permanent Taklimakan Desert linked to the mid-Pleistocene transition

Weiguo Liu[1,2], Zhonghui Liu[3]*, Jimin Sun[2,4,5], Chunhui Song[6], Hong Chang[1], Huanye Wang[1], Zheng Wang[1] and Zhisheng An[1,2]*

[1]State Key Laboratory of Loess and Quaternary Geology, Institute of Earth Environment, Center for Excellence in Quaternary Science and Global Change, Chinese Academy of Sciences, 710061 Xi'an, China
[2]University of Chinese Academy of Sciences, Beijing 100049, China
[3]Department of Earth Sciences, The University of Hong Kong, Hong Kong, China
[4]Key Laboratory of Cenozoic Geology and Environment, Institute of Geology and Geophysics, Chinese Academy of Sciences (CAS), Beijing 100029, China
[5]CAS Center for Excellence in Tibetan Plateau Earth Sciences, Chinese Academy of Sciences, Beijing 100101, China
[6]Key Laboratory of Western China's Mineral Resources of Gansu Province & School of Earth Sciences, Lanzhou University, Lanzhou 730000, China

ABSTRACT

The initial occurrence of desert landscape or eolian sand dunes is thought to have occurred long before the Pleistocene, and desertification was subsequently enhanced under cold, dusty glacial conditions. However, when and how the desert landscape persisted during both glacial and interglacial periods, defined as "permanent" desert here, remain elusive. Here, we present carbonate carbon isotope and grain-size records from the Tarim Basin, western China, revealing a detailed desertification history for the Taklimakan Desert. Our records demonstrate that after desiccation of episodic lakes at ca. 4.9 Ma, alternations of eolian sand dunes and fluvial and playa-like conditions persisted for a long period until 0.7 Ma in the Tarim Basin. The onset of permanent desert landscape around 0.7–0.5 Ma occurred concurrently with the climatic reorganization across the mid-Pleistocene transition. The occurrence of mountain glaciers on the Tibetan Plateau and atmospheric circulation changes may have controlled the formation and extreme aridification of the permanent desert in inland Asia since the mid-Pleistocene transition.

INTRODUCTION

Long, continuous terrestrial records documenting inland aridity changes are extremely limited, preventing our understanding of the development of aridification and desertification in continent inland areas and their association with Pliocene–Pleistocene global climatic changes. The Taklimakan Desert in the Tarim Basin, western China (Fig. 1), the second largest shifting-sand desert in the world, is part of the prominent arid zone in Central Asia. Today, extremely dry climate prevails in the basin (annual precipitation < 50 mm at its center), and shifting sand dunes occupy most of the basin, with little vegetation (Zhu et al., 1980). Summer subtropical anticyclone and air subsidence there are thought to be remotely forced by the rising activity in monsoon regions (Rodwell and Hoskins, 1996; Sato and Kimura, 2005). A detailed aridification history over the Pliocene–Pleistocene period from this region, which is perhaps most representative of inland aridity changes around the globe, would help us to understand monsoon-desert dynamics in response to global climatic changes.

Although it has been extensively studied over the past decades, the timing and mechanisms of Taklimakan Desert formation still remain elusive. The proposed timing, mostly based on the initial occurrence of eolian deposits, ranges from the Pleistocene to Miocene and late Oligocene (Zhu et al., 1980; Fang et al., 2002a; Sun et al., 2009; Zheng et al., 2015; Heermance et al., 2018). Proposed possible mechanisms for Asian inland aridification, and by inference, desertification, include tectonic uplift (Fang et al., 2002a), land-sea distributions (Bosboom et al., 2014), and Cenozoic global cooling (Miao et al., 2012). It is generally believed that the initial desert landscape occurred well before the Pleistocene, and desertification was enhanced under cold, dusty Pleistocene glacial conditions. However, little is known about when and how the desert ceased being replaced by other landscapes during relatively warm, humid interglacial periods, such as the present Holocene period, defined as "permanent" desert, which is addressed here.

METHOD

We used a 1050-m-long, continuous borehole (Ls2) that we drilled at Lop Nur (39°46′0″N, 88°23′19″E) in the eastern Tarim Basin (Fig. 1). Previous studies have established a robust chronology (Fig. S1A in the Supplemental Material[1]; Chang et al., 2012), and, through study of the lower section of the core (651–1050 m), inferred the occurrence of late Miocene episodic lakes, based on carbonate oxygen and boron isotopes (Liu et al., 2014). We here addressed how the Taklimakan Desert evolved into its present form after the episodic lakes dried up at ca. 4.9 Ma (Liu et al., 2014; Sun et al., 2017). Existing

*E-mails: zhliu@hku.hk; anzs@loess.llqg.ac.cn.

[1]Supplemental Material. Materials, methods, and interpretations, Figure S1 (stratigraphic columns and age assignments), Figure S2 ($\delta^{13}C$ correlated with rainfall and temperature), Figure S3 (detailed view of the onset of desertification), Figure S4 (representative core photos), Figure S5 (Lop Nur and Mazartag $\delta^{13}C$), Figure S6 (spectral results), Figure S7 (close-up views of records), and Table S1 ($\delta^{18}O$, $\delta^{13}C$, and grain-size data). Please visit https://doi.org/10.1130/GEOL.26213S.12221885 to access the supplemental material, and contact editing@geosociety.org with any questions.

CITATION: Liu, W., et al., 2020, Onset of permanent Taklimakan Desert linked to the mid-Pleistocene transition: Geology, v. 48, p. 782–786, https://doi.org/10.1130/G47406.1

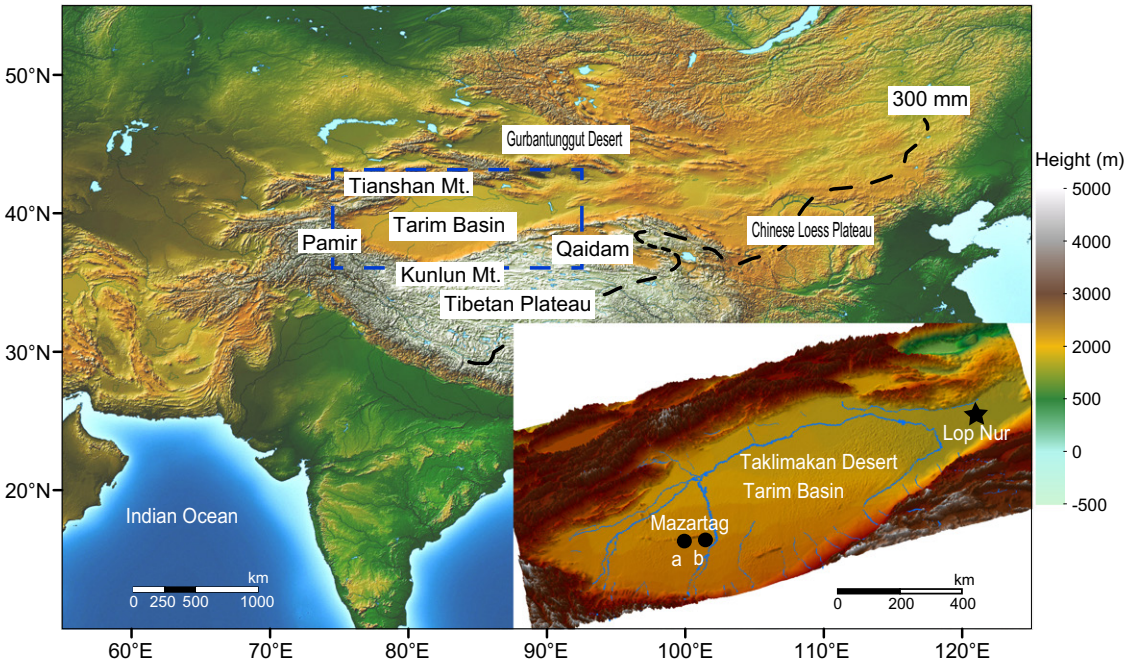

Figure 1. Geographic locations of the studied Lop Nur and Mazartag profiles in the Tarim Basin, western China. Base topographic map was generated with ArcGIS software. The Tarim Basin is currently surrounded by high mountains with average elevations >4000 m. Dashed line is 300 mm annual precipitation line, which roughly separates the Asian inland from monsoonal regions. Inset map shows locations of Lop Nur borehole (star), upper Mazartag (a) and lower Mazartag (b) sections, and river system in Tarim Basin.

records from exposed Mazartag sections in the central basin (Fig. 1; Pei et al., 2011; Sun et al., 2017), where previously controversial age assignments have been reconciled with a newly reported mammal fossil (Fig. S1C; Sun et al., 2017), were also integrated to infer basinwide paleoenvironmental changes. Lop Nur currently lies at the lowest elevation in the eastern basin, ~800 m above sea level, and is terminal for receiving river water in the basin, and the Mazartag sections are at ~1150 m in the central basin (Fig. 1), so the borehole at Lop Nur would likely record the last stage of aridity changes in the basin, while approximately synchronous signals at both locations could indicate major, basinwide paleoenvironmental changes.

We generated carbonate carbon isotope ($\delta^{13}C_{carb}$) and grain-size records at very high resolution (<2 k.y. on average; Table S1). The $\delta^{13}C_{carb}$ values from eolian and fluvial deposits can become progressively negative with the input of soil organic carbon during soil pedogenesis (see the Supplemental Material, and Fig. S2; Liu et al., 2011; Sun et al., 2015; Caves et al., 2016). Hence, $\delta^{13}C_{carb}$ can effectively reflect regional vegetation cover and biological productivity in arid and semiarid regions. Grain size, due to its complicated nature, is used here as a supporting indicator (see the Supplemental Material). However, when desert landscape occurs, the sand fraction should dominate the size distribution. Using the two indicators, we defined the onset of "permanent" desert formation as the point at which $\delta^{13}C_{carb}$ consistently fell within 0‰ ± 1‰ and modal size, the mostly frequent occurring particle size, was >~100 µm, both similar to those in modern Taklimakan sand. Analytical procedures for $\delta^{18}O_{carb}$, $\delta^{13}C_{carb}$, and grain-size analyses can be found in the Supplemental Material.

RESULTS AND DISCUSSION

Our $\delta^{13}C_{carb}$ record over the past 7.1 m.y. shows a long-term trend toward more positive values, with large variability between ~1‰ and −5‰ (Fig. 2B). After the episodic lacustrine phase, as evidenced by the high variability in $\delta^{18}O_{carb}$ between 7.1 and 4.9 Ma (Fig. 2D; Liu et al., 2014), $\delta^{13}C_{carb}$ values ranged from ~0‰ to −5‰ between 4.9 and 3 Ma, and from ~1‰ to −3‰ with a trend becoming progressively positive between 3 and 0.7 Ma. Since ca. 0.7 Ma, $\delta^{13}C_{carb}$ values stayed around 0‰ ±1‰, close to the background signal in detrital carbonates (Liu et al., 2014). The grain-size record (Fig. 2C) also shows large variability in modal size, from 5–10 µm to 100–150 µm before ca. 0.5 Ma. An abrupt increase occurred at ca. 0.5 Ma, and since then, the modal size has varied between ~100 and 200 µm (Fig. 2C; Fig. S3). Notably, after the mid-Pleistocene transition (MPT) between ca. 1.25

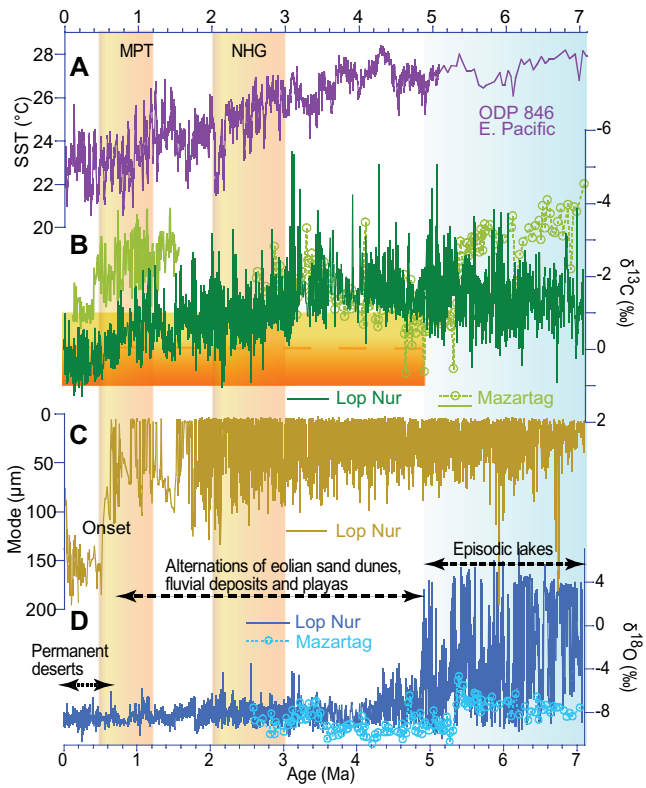

Figure 2. Proxy records over past 7.1 m.y. in the Tarim Basin, western China. (A) Sea-surface temperature (SST) record from Ocean Drilling Program (ODP) Site 846 in the eastern equatorial Pacific (Herbert et al., 2016). (B) $\delta^{13}C_{carb}$, (C) grain size, and (D) $\delta^{18}O_{carb}$ from the Lop Nur borehole (this study; Liu et al., 2014) and Mazartag sections (Pei et al., 2011; Sun et al., 2017). NHG—Northern Hemisphere glaciation; MPT—mid-Pleistocene transition. Horizontal dashed line and bar in B highlight range of $\delta^{13}C_{carb}$ values (0‰ ± 1‰) in detrital carbonates, interpreted as minimal vegetation cover.

and 0.7 Ma (Clark et al., 2006), both $\delta^{13}C_{carb}$ and modal size show little glacial-interglacial variability, which indicates persistent desert landscape during both glacial and interglacial periods.

We also closely examined lithological changes (Figs. S3 and S4). Prior to ca. 4.9 Ma (651 m), the occurrence of gray and bluish gray argillaceous limestone suggests lacustrine environments. After that, the sediment gradually changed from gray and bluish-gray to yellow/brown color, with an increasing silt component. Since ca. 0.7 Ma (34 m), sediments mainly consist of coarse sand, with little soil pedogenesis developed. Thus, the $\delta^{13}C_{carb}$ and grain-size records (Figs. 2B and 2C), together with lithological changes (Figs. S3 and S4), indicate three desertification stages in the Tarim Basin: episodic lakes before ca. 4.9 Ma (Liu et al., 2014), alternations of eolian sand dunes, fluvial deposits, and playas (Fig. 2D) between ca. 4.9 Ma and 0.7 Ma, and "permanent" desert landscape after 0.7 Ma.

The $\delta^{13}C_{carb}$ records from exposed Mazartag sections in the central basin (Pei et al., 2011; Sun et al., 2017), 700 km away from our Lop Nur borehole, confirm that the Lop Nur profiles represent basinwide paleoenvironmental changes. In the lower Mazartag section, substantially increased $\delta^{13}C_{carb}$ and decreased $\delta^{18}O_{carb}$ values (Figs. 2B and 2D) indicate lake desiccation at ca. 5.3 Ma at this locality (Sun et al., 2017). Between 4.9 and 2.6 Ma, the two profiles display similar $\delta^{13}C_{carb}$ variability. Although $\delta^{13}C_{carb}$ values are more negative in the upper Mazartag section (1.6–0.1 Ma; Fig. 2B; Fig. S5), the pattern of $\delta^{13}C_{carb}$ variations in the two profiles is quite similar, with both gradually becoming more positive and an abrupt increase in $\delta^{13}C_{carb}$ values at ca. 0.7 or 0.4 Ma (Fig. S5). Further, both lithological columns show coarsening-upward trends around the MPT (Figs. S1A and S1B). The similar $\delta^{13}C_{carb}$ values and lithological changes in the two profiles allow us to place the onset of modern-form permanent Taklimakan Desert at 0.7–0.5 Ma.

The high variability before ca. 0.7 Ma in both $\delta^{13}C_{carb}$ and grain-size records appears to have been associated with glacial-interglacial changes. Spectral analysis confirms the presence of variability at orbital bands, particularly at ~400 k.y. (Fig. S6). More negative $\delta^{13}C_{carb}$ values and smaller grain size occurred during interglacial periods, while the opposite took place during glacial periods (Figs. S7A and S7B). The extremely negative $\delta^{13}C_{carb}$ values (–3‰ to –5‰) seem to have occurred, within chronological uncertainty, ~400 k.y. apart. Hence, as indicated by the glacial $\delta^{13}C_{carb}$ value (0‰ ± 1‰) and large modal size (~100–200 µm; Figs. 2B and 2C), brief desert landscapes could have occurred much earlier, not inconsistent with the various timing inferred previously (Zhu et al., 1980; Fang et al., 2002a; Sun et al., 2009, 2017; Liu et al., 2014; Zheng et al., 2015; Heermance et al., 2018). However, all these brief desert occurrences were replaced by substantial interglacial vegetation cover before 0.7 Ma, as shown by interglacial $\delta^{13}C_{carb}$ values (–2‰ to –5‰) and much smaller modal sizes (5–10 µm). The gradual deterioration of vegetation during the MPT (1.25–0.7 Ma) but subsequent abrupt increase in modal size at ca. 0.5 Ma (Figs. 3F and 3G; Fig. S7C) may suggest that the permanent desert landscape could have fully formed only when a certain vegetation cover threshold was crossed through a positive vegetation (albedo) feedback in desert dynamics (Abell et al., 2020). It remains to be verified whether "permanent" desert landscapes in other Asian inland deserts developed around the same time; however, substantially enhanced aridification around the MPT time has also been reported in the Qaidam Basin (Cai et al., 2012), Gurbantunggut Desert (Fang et al., 2002b), and the west margin of the Tarim Basin (Zhang et al., 2019), largely consistent with the permanent Taklimakan Desert formation at 0.7–0.5 Ma inferred here.

Our high-resolution Lop Nur profiles show close correspondence to Pliocene–Pleistocene global climatic changes before 0.7 Ma (Fig. 2; Fig. S7). During glacial/cool periods, minimal vegetation cover in the basin occurred while Asian summer monsoons also weakened (Sun et al., 2010). During interglacial periods at ca. 1.2, 2.0, 2.4, and 2.8 Ma, marked increase in vegetation cover in the basin coincided with enhanced East Asian summer monsoons (Fig. S7A). Supported by model simulations (An et al., 2001), glacial conditions or cool global temperatures tend to enhance aridity in both Asian inland and monsoonal regions. The close correspondence between synchronous aridity changes in both monsoon and desert regions and large global climatic changes after ca. 3 Ma (Fig. 2; Fig. S7) leaves the role of tectonic uplift dispensable. In addition, the high elevations (>3000 m) of the Tibetan Plateau were attained at least by the latest Miocene (Molnar, 2005), and no firm evidence exists for marked uplift after ca. 3 Ma (Clift et al., 2017). We thus suggest that global climatic changes, the long-term cooling trend in particular, were largely responsible for the deteriorating vegetation cover in the Tarim Basin between ca. 3 and 0.7 Ma.

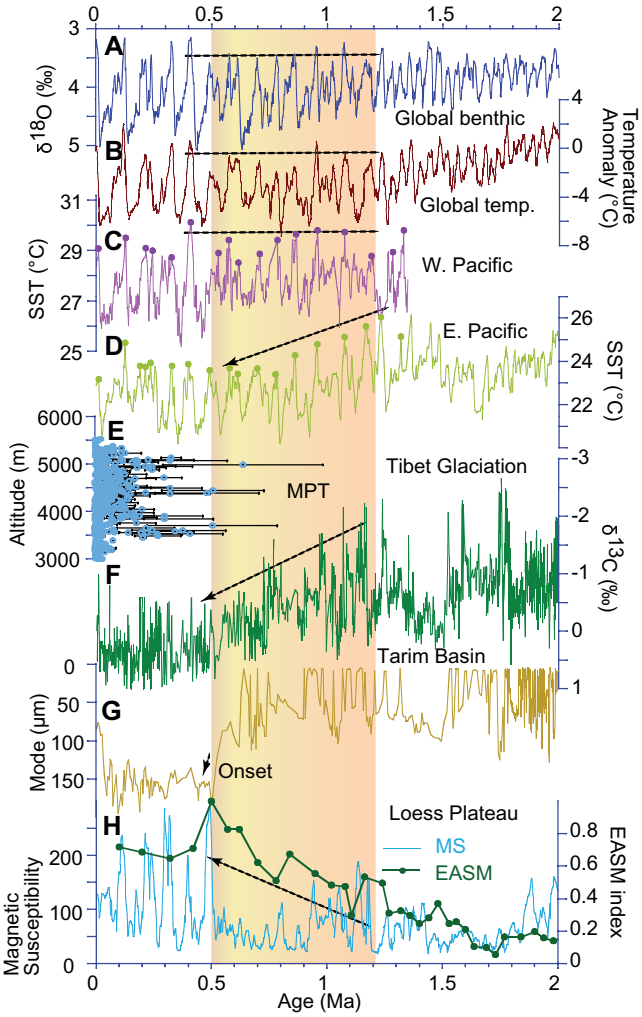

Figure 3. Detailed desertification history over past 2 m.y., compared with other relevant records. (A) Global benthic $\delta^{18}O$ stack (Lisiecki and Raymo, 2005). (B) Global average surface temperature (GAST) change (Snyder, 2016). (C,D) Tropical sea-surface temperature (SSTs) in the western Pacific Oean (Ocean Drilling Program [ODP] Site 806; Medina-Elizalde and Lea, 2005) and eastern Pacific (ODP Site 846; Herbert et al., 2010), with interglacial maxima highlighted. (E) Synthesized ages of mountain glaciation on the Tibetan Plateau (Heyman, 2014) plotted against altitude (>3000 m), with dating uncertainty indicated. (F,G) $\delta^{13}C_{carb}$ and grain size from the Lop Nur profile (Tarim Basin, western China). (H) Magnetic susceptibility (MS; in units of 10^{-8} m^3 kg^{-1}; Sun et al., 2010) and East Asian summer monsoon (EASM) rainfall index (Meng et al., 2018) from the Chinese Loess Plateau. Dashed lines indicate respective trend for interglacial periods across mid-Pleistocene transition.

However, the onset of the permanent desert landscape, around 0.7–0.5 Ma (Figs. 2B and 2C), is difficult to explain by the global cooling effect. The MPT was characterized by further cooling and ice-sheet development during glacial periods (Fig. 3A; Clark et al., 2006), yet interglacial temperatures around the globe (Snyder, 2016) and in western tropical Pacific Ocean (Medina-Elizalde and Lea, 2005) remained about the same (Figs. 3B and 3C). One of the prominent regional features during the MPT was that mountain glaciers started to occur on the Tibetan Plateau and surrounding mountains (Heyman, 2014; Owen and Dortch, 2014), approximately coincident with the permanent desert formation (Fig. 3E). Mountain glaciation, through enhanced frost weathering and/or glacial grinding, would intensify physical weathering and rock breaks, thus generating more sand-sized materials (Smalley, 1995) for sustaining a permanent large desert. We suggest that the recurrent advance and retreat of mountain glaciers, corresponding to glacial-interglacial cycles, provided tremendous volumes of sand for the formation of the permanent desert in the Tarim Basin since ca. 0.5 Ma.

Intriguingly, there exists some indication that the East Asian (Sun et al., 2010; Meng et al., 2018) and Indian summer monsoons (An et al., 2001; Huang et al., 2007) were more enhanced during interglacial periods after the MPT than before (Fig. 3H), while in the Tarim Basin, interglacial aridity increased after the MPT as compared to before the MPT (Figs. 3F and 3G). Mountain glaciation could have increased aridity in both desert and monsoon regions (An et al., 2001), but this could not explain the opposite aridity behavior for interglacial periods after ca. 0.7 Ma. Instead, because air subsidence and thus suppressed rainfall in desert regions are remotely enhanced by diabatic heating over Asian monsoon regions (Rodwell and Hoskins, 1996; Sato and Kimura, 2005), this monsoon-desert mechanism could well explain the opposite aridity behavior for interglacial periods after the MPT in the two regions (Figs. 3F–3H). Previously, the enhanced interglacial summer monsoon across the MPT (Meng et al., 2018) has been linked to a greater tropical zonal temperature gradient and strengthened Walker Circulation (Wara et al., 2005), as interglacial temperatures continued to cool in the eastern equatorial Pacific (Herbert et al., 2010) but remained stable in the western Pacific (Figs. 3C and 3D; Medina-Elizalde and Lea, 2005). Accordingly, we suggest that in response to strengthened monsoon circulation across the MPT, air subsidence was enhanced in desert regions through the monsoon-desert dynamics (Rodwell and Hoskins, 1996). Hence, further reorganization of atmospheric circulation around the MPT may have also contributed to the onset of the permanent Taklimakan Desert, which requires further investigation with climate models.

In summary, our high-resolution $\delta^{13}C_{carb}$ and grain-size records over the past 7.1 m.y. from the borehole at Lop Nur provide a detailed desertification history in the Tarim Basin, western China. Our results show the onset of the "permanent" Taklimakan Desert at 0.7–0.5 Ma, when desert landscape persisted during both glacial and interglacial periods. The overall deteriorating vegetation cover between 3 Ma and 0.7 Ma in the Tarim Basin corresponded to global cooling, but the onset of permanent desert at 0.7–0.5 Ma appears to have been linked to the mountain glaciation in nearby regions and atmospheric circulation changes across the MPT.

ACKNOWLEDGMENTS

We thank the editor and four anonymous reviewers for their constructive reviews. This research was supported by the Chinese Academy of Sciences (grants XDB40010100, XDA20070202, and QYZDY-SSW-DQC001), the National Natural Science Foundation of China (grant 41420104008), and the National Key Research and Development Program of China (grant 2016YFE0109500). The Lop Nur Drilling Project was supported by the Chinese Academy of Sciences.

REFERENCES CITED

Abell, J.T., Pullen, A., Lebo, Z.J., Kapp, P., Metcalf, A.R., Nie, J., and Winckler, G., 2020, A wind-albedo-wind feedback driven by landscape evolution: Nature Communications, v. 11, p. 96, https://doi.org/10.1038/s41467-019-13661-w.

An, Z., Kutzbach, J.E., Prell, W.L., and Porter, S.C., 2001, Evolution of Asian monsoons and phased uplift of the Himalaya–Tibetan Plateau since late Miocene times: Nature, v. 411, p. 62–66, https://doi.org/10.1038/35075035.

Bosboom, R., Dupont-Nivet, G., Grothe, A., Brinkhuis, H., Villa, G., Mandic, O., Stoica, M., Kouwenhoven, T., Huang, W., Yang, W., and Guo, Z., 2014, Timing, cause and impact of the late Eocene stepwise sea retreat from the Tarim Basin (west China): Palaeogeography, Palaeoclimatology, Palaeoecology, v. 403, p. 101–118, https://doi.org/10.1016/j.palaeo.2014.03.035.

Cai, M., Fang, X., Wu, F., Miao, Y., and Appel, E., 2012, Pliocene–Pleistocene stepwise drying of Central Asia: Evidence from paleomagnetism and sporopollen record of the deep borehole SG-3 in the western Qaidam Basin, NE Tibetan Plateau: Global and Planetary Change, v. 94–95, p. 72–81, https://doi.org/10.1016/j.gloplacha.2012.07.002.

Caves, J.K., Moragne, D.Y., Ibarra, D.E., Bayshashov, B.U., Gao, Y., Jones, M.M., Zhamangara, A., Arzhannikova, A.V., Arzhannikov, S.G., and Chamberlain, C.P., 2016, The Neogene de-greening of Central Asia: Geology, v. 44, p. 887–890, https://doi.org/10.1130/G38267.1.

Chang, H., An, Z., Liu, W., Qiang, X., Song, Y., and Ao, H., 2012, Magnetostratigraphic and paleoenvironmental records for a Late Cenozoic sedimentary sequence drilled from Lop Nur in the eastern Tarim Basin: Global and Planetary Change, v. 80–81, p. 113–122.

Clark, P.U., Archer, D., Pollard, D., Blum, J.D., Rial, J.A., Brovkin, V., Mix, A.C., Pisias, N.G., and Roy, M., 2006, The middle Pleistocene transition: Characteristics, mechanisms, and implications for long-term changes in atmospheric pCO_2: Quaternary Science Reviews, v. 25, p. 3150–3184, https://doi.org/10.1016/j.quascirev.2006.07.008.

Clift, P.D., Zheng, H., Carter, A., Böning, P., Jonell, T.N., Schorr, H., Shan, X., Pahnke, K., Wei, X., and Rittenour, T., 2017, Controls on erosion in the western Tarim Basin: Implications for the uplift of northwest Tibet and the Pamir: Geosphere, v. 13, p. 1747–1765, https://doi.org/10.1130/GES01378.1.

Fang, X., Lü, L., Yang, S., Li, J., An, Z., Jiang, P., and Chen, X., 2002a, Loess in Kunlun Mountains and its implications on desert development and Tibetan Plateau uplift in west China: Science in China, ser. D, Earth Sciences, v. 45, p. 289–299, https://doi.org/10.1360/02yd9031.

Fang, X., Shi, Z., Yang, S., Yan, M., Li, J., and Jiang, P., 2002b, Loess in the Tian Shan and its implications for the development of the Gurbantunggut Desert and drying of northern Xinjiang: Chinese Science Bulletin, v. 47, p. 1381–1387, https://doi.org/10.1360/02tb9305.

Heermance, R.V., Pearson, J., Moe, A., Liu, L., Xu, J., Chen, J., Richter, F., Garzione, C.N., Nie, J., and Bogue, S., 2018, Erg deposition and development of the ancestral Taklimakan Desert (western China) between 12.2 and 7.0 Ma: Geology, v. 46, p. 919–922, https://doi.org/10.1130/G45085.1.

Herbert, T.D., Peterson, L.C., Lawrence, K.T., and Liu, Z., 2010, Tropical ocean temperatures over the past 3.5 million years: Science, v. 328, p. 1530–1534, https://doi.org/10.1126/science.1185435.

Herbert, T.D., Lawrence, K.T., Tzanova, A., Peterson, L.C., Caballero-Gill, R., and Kelly, C.S., 2016, Late Miocene global cooling and the rise of modern ecosystems: Nature Geoscience, v. 9, p. 843–847, https://doi.org/10.1038/ngeo2813.

Heyman, J., 2014, Paleoglaciation of the Tibetan Plateau and surrounding mountains based on exposure ages and ELA depression estimates: Quaternary Science Reviews, v. 91, p. 30–41, https://doi.org/10.1016/j.quascirev.2014.03.018.

Huang, Y., Clemens, S.C., Liu, W., Wang, Y., and Prell, W.L., 2007, Large-scale hydrological change drove the late Miocene C_4 plant expansion in the Himalayan foreland and Arabian Peninsula: Geology, v. 35, p. 531–534, https://doi.org/10.1130/G23666A.1.

Lisiecki, L.E., and Raymo, M.E., 2005, A Pliocene–Pleistocene stack of 57 globally distributed benthic $\delta^{18}O$ records: Paleoceanography, v. 20, PA1003, https://doi.org/10.1029/2004PA001071.

Liu, W., Yang, H., Sun, Y., and Wang, X., 2011, $\delta^{13}C$ values of loess total carbonate: A sensitive proxy for Asian monsoon rainfall gradient in arid northwestern margin of the Chinese Loess Plateau: Chemical Geology, v. 284, p. 317–322, https://doi.org/10.1016/j.chemgeo.2011.03.011.

Liu, W., Liu, Z., An, Z., Sun, J., Chang, H., Wang, N., Dong, J., and Wang, H., 2014, Late Miocene episodic lakes in the arid Tarim Basin, western China: Proceedings of the National Academy of Sciences of the United States of America, v. 111, p. 16292–16296, https://doi.org/10.1073/pnas.1410890111.

Medina-Elizalde, M., and Lea, D.W., 2005, The mid-Pleistocene transition in the tropical Pacific: Science, v. 310, p. 1009–1012, https://doi.org/10.1126/science.1115933.

Meng, X., Liu, L., Wang, X.T., Balsam, W., Chen, J., and Ji, J., 2018, Mineralogical evidence of reduced East Asian summer monsoon rainfall on the Chinese Loess Plateau during the early Pleistocene interglacials: Earth and Planetary Science Letters, v. 486, p. 61–69, https://doi.org/10.1016/j.epsl.2017.12.048.

Miao, Y., Herrmann, M., Wu, F., Yan, X., and Yang, S., 2012, What controlled mid–late Miocene long-term aridification in Central Asia?—Global cooling or Tibetan Plateau uplift: A review: Earth-

Science Reviews, v. 112, p. 155–172, https://doi.org/10.1016/j.earscirev.2012.02.003.
Molnar, P., 2005, Mio-Pliocene growth of the Tibetan Plateau and evolution of East Asian climate: Palaeontologia Electronica, v. 8, p. 2A.
Owen, L.A., and Dortch, J.M., 2014, Nature and timing of Quaternary glaciation in the Himalayan-Tibetan orogeny: Quaternary Science Reviews, v. 88, p. 14–54, https://doi.org/10.1016/j.quascirev.2013.11.016.
Pei, J., Li, H., Si, J., Pan, J., Wu, F., Sun, Z., and Zhao, Y., 2011, The response of the Tibet uplift since the early Pleistocene in the centre of Tarim Basin: Acta Petrologica Sinica (Yanshi Xuebao), v. 27, p. 3487–3498 [in Chinese with English abstract].
Rodwell, M.J., and Hoskins, B.J., 1996, Monsoons and the dynamics of deserts: Quarterly Journal of the Royal Meteorological Society, v. 122, p. 1385–1404, https://doi.org/10.1002/qj.49712253408.
Sato, T., and Kimura, F., 2005, Impact of diabatic heating over the Tibetan Plateau on subsidence over northeast Asian arid region: Geophysical Research Letters, v. 32, L05809, https://doi.org/10.1029/2004GL022089.
Smalley, I.J., 1995, Making the material: The formation of silt sized primary mineral particles for loess deposits: Quaternary Science Reviews, v. 14, p. 645–651, https://doi.org/10.1016/0277-3791(95)00046-1.
Snyder, C.W., 2016, Evolution of global temperature over the past two million years: Nature, v. 538, p. 226–228, https://doi.org/10.1038/nature19798.
Sun, J., Liu, W., Liu, Z., Deng, T., Windley, B.F., and Fu, B., 2017, Extreme aridification since the beginning of the Pliocene in the Tarim Basin, western China: Palaeogeography, Palaeoclimatology, Palaeoecology, v. 485, p. 189–200, https://doi.org/10.1016/j.palaeo.2017.06.012.
Sun, J.M., Zhang, Z.Q., and Zhang, L.Y., 2009, New evidence on the age of the Taklimakan Desert: Geology, v. 37, p. 159–162, https://doi.org/10.1130/G25338A.1.
Sun, Y., An, Z., Clemens, S.C., Bloemendal, J., and Vandenberghe, J., 2010, Seven million years of wind and precipitation variability on the Chinese Loess Plateau: Earth and Planetary Science Letters, v. 297, p. 525–535, https://doi.org/10.1016/j.epsl.2010.07.004.
Sun, Y., Kutzbach, J., An, Z., Clemens, S., Liu, Z., Liu, W., Liu, X., Shi, Z., Zheng, W., Liang, L., Yan, Y., and Li, Y., 2015, Astronomical and glacial forcing of East Asian summer monsoon variability: Quaternary Science Reviews, v. 115, p. 132–142, https://doi.org/10.1016/j.quascirev.2015.03.009.
Wara, M.W., Ravelo, A.C., and Delaney, M.L., 2005, Permanent El Niño–like conditions during the Pliocene warm period: Science, v. 309, p. 758–761, https://doi.org/10.1126/science.1112596.
Zhang, R., Li, L., Gu, Y., Huang, C., Ogg, J., Li, Q., Lu, C., and Wang, Z., 2019, Astronomical forcing of terrestrial climate recorded in the Pleistocene of the western Tarim Basin, NW China: Palaeogeography, Palaeoclimatology, Palaeoecology, v. 530, p. 78–89, https://doi.org/10.1016/j.palaeo.2019.05.039.
Zheng, H., Wei, X., Tada, R., Clift, P.D., Wang, B., Jourdan, F., Wang, P., and He, M., 2015, Late Oligocene – early Miocene birth of the Taklimakan Desert: Proceedings of the National Academy of Sciences of the United States of America, v. 112, p. 7662–7667, https://doi.org/10.1073/pnas.1424487112.
Zhu, Z.D., Wu, Z., Liu, S., and Di, X.M., eds., 1980, An Outline of Chinese Deserts: Beijing, Science Press, 107 p. [in Chinese].

Printed in USA